



# Key parameters influencing performance and failure modes for interaction soil–pile–structure system under lateral loading

Gasmi Houda<sup>1</sup> · Bouzid Tayeb<sup>1</sup> · D. Yahiaoui<sup>1</sup>

Received: 6 November 2017 / Accepted: 6 March 2018 / Published online: 20 March 2018  
© Springer International Publishing AG, part of Springer Nature 2018

## Abstract

The behavior of the interaction soil–pile–structure under lateral loads is a topic not fully investigated in the literature. However, soil–pile–superstructure interaction largely affects the design forces in columns and piles. In contrast, fixed base assumption cannot capture soil structure interaction effect. In this study, the effects of the lateral capacity of interaction soil–pile–structure (ISPS) system under lateral loads have been investigated. The lateral capacity of ISPS system can be obtained by pushover analysis. The influence of vertical loads, pile diameter, longitudinal steel ratio, length of pile and type of soil on the lateral response of piles installed in three types of sandy soil are brought out in this paper through nonlinear static analysis and pile behavior in these conditions is investigated and characterized via: lateral capacity, spectral capacity, performance point, position of plastic hinge, over-strength factor, ductility and the response modification factors. The results indicate that the lateral capacity and spectral capacity are affected.

**Keywords** Interaction soil–pile–structure · Lateral capacity · Plastic hinge · Ductility · Response modification factor · Pushover analysis

## Introduction

In practice, the structures are generally considered fixed at base for seismic analysis and design. The structure and pile are separated to account for the effect of soil–pile/structure and structure/soil–pile. In fact, the seismic interaction soil–pile structure (ISPS) is usually considered beneficial to structure system under seismic loading because it stretches the period of structure and hence increases the damping of the structural system. Thus, considering the ISPS tends to reduce the base shear, and in turn the structure demand, of the superstructure in comparison with the fixed-based case. In contrast, the increase in the overall displacement of the superstructure in comparison to the fixed-base condition due to translation and rotation of the foundation (e.g. Guin and Banerjee 1998; Yingcai 2002) can change the performance level of the structure. Moreover, increase in the total

deformation of structure, and in turn secondary  $P$ – $\Delta$  effect, influences the overall stability of the structure (Fig. 1).

In conventional seismic design, piles are designed to be elastic because it is more convenient to have plasticity occurring in the superstructure without any damage to its foundation or near the ground surface for accessible inspection and repair. Elastic response of the foundation can be ensured by increasing the strength of the foundation above that of the bridge pier so that plastic hinging occurs in the pier instead of the foundation.

But the foundation design is cost-effective when compared to the column/pile-cap/pile combination since the construction of an expensive pile-cap can be eliminated. However, the damage inspection after an earthquake, extensive yielding of the pile below the ground level might result in an unacceptable level of residual displacement, which may render the structure unserviceable after an earthquake. In addition to the difficulty in the response of a laterally loaded pile, there is a complicated soil–structure interaction problem. This is because pile deflection depends on soil reaction and in turn soil reaction is influenced by pile deflection.

✉ Gasmi Houda  
houda\_gasmi@yahoo.com

<sup>1</sup> Department of Civil Engineering, University of Batna 2, Batna, Algeria

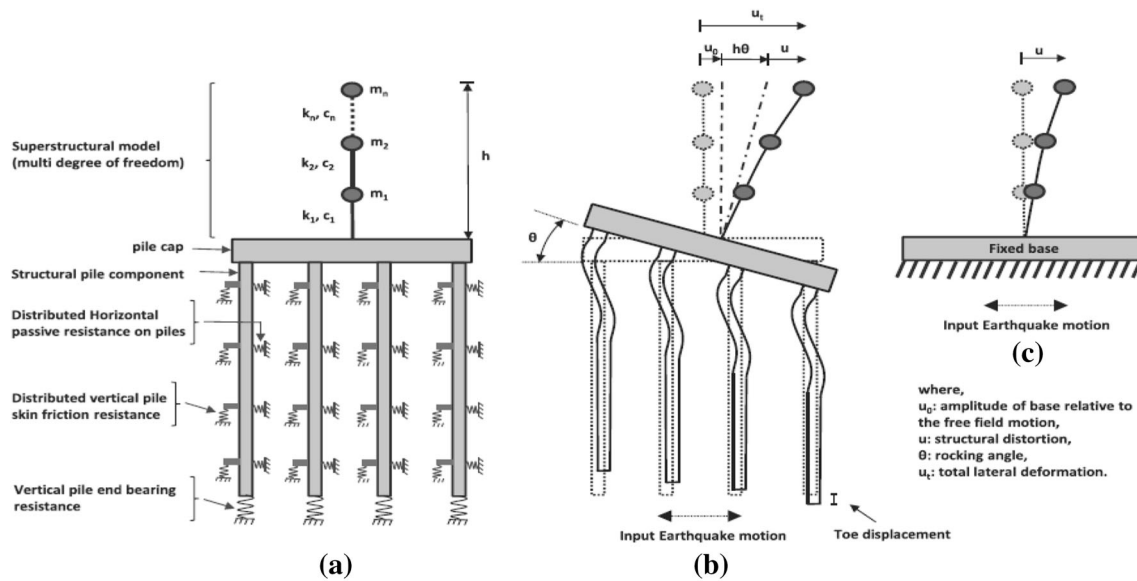


**Fig. 1** Schematic modeling of the multi degree freedom structure considering: **a** structure supported by floating pile foundation employing foundation springs; **b** lateral deformation and rocking of

the structure supported by floating pile foundation; **c** lateral deformation of the fixed-base structure

Many researchers have investigated the influence of axial loads on the response of laterally loaded pile. Some have insisted that the effect of axial compression load is of minor importance and can be neglected in the design. Although the opposite view of axial force effects on the lateral pile response was formed by other researchers.

The performance of structure above piles depends widely on the behavior of pile foundation under earthquake loading. The lateral stiffness, strength and ductility capacity of the pile depend on the amount and details of the longitudinal and transverse reinforcement, and to a lesser extent, the compressive strength of the concrete. The lateral force–deformation characteristics of the pile also depend on the interaction between the pile and surrounding soil. For most structure, however, the inertial force from superstructure tends to dominate the inelastic deformation of pile.

Many studies of the behavior of pile–soil interaction by either experimental tests or numerical analyses have been made without taking into consideration the super-structure under the static loading (Chiou and Chen 2010; Chiou et al. 2012; Karthigeyan et al. 2006, 2007; Khodair and Abdel-Mohti 2014; Chiou et al. 2009). This study aims to present a numerical investigation to understand and highlight the effect of sand soil types, pile length, pile diameter, longitudinal steel ratio, and axial force level on lateral capacity of soil–pile–structure system and the performance of structure. Finally, a number of numerical pushover analyses (capacity spectrum and inelastic demand spectrum methods) based on the nonlinear Winkler-beam model are conducted to illustrate the effect of previous items on

lateral capacity and performance point, formation of plastic hinge, over-strength factor, ductility and the response modification factors.

## Model analysis

The numerical analyses developed and described in this paper with different nonlinear modeling strategies were studied using the computer program Sap2000 (2002). The program includes models for the representation of the behavior of spatial frames, pile, and soil to simulate the behavior of ISPS, under static and/or dynamic loading, considering both material and geometric nonlinearities. In this research study, the pushover analysis is used in simulating the nonlinear response of structure, pile and soil. The following modeling's considerations are made:

### Modeling superstructure and pile nonlinearity

Nonlinear analysis, either static or dynamic, needs a detailed modeling of the regions of the structure where inelastic deformations are expected to be developed. Two approaches can be adopted, the plastic hinge or the fiber approach. The Interaction PMM Hinge as shown in Fig. 2 is used to simulate the pile and column nonlinearity and the lumped-plasticity (the so-called plastic-hinge). The configuration of the column cross section must be taken into account in a separate moment–curvature analysis and interaction diagram, carried out to determine the nominal capacity  $M_{ne}$ , plastic capacity  $M_p$ , and ultimate capacity  $M_u$

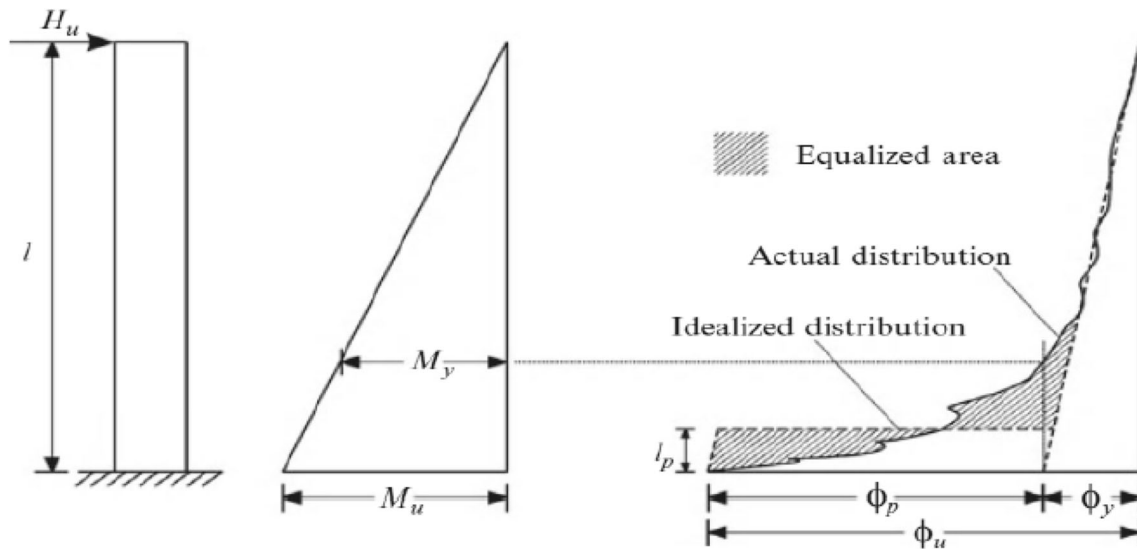


**Fig. 2** Equivalent column and the definition of the equivalent plastic hinge based on the idealized curvature distribution

of the column, as well as the rotations ( $\theta$ ) or curvatures ( $\phi$ ) related to those values, in discrete bending directions of the column.

The elastic stiffness of the column section is used until the yield point or nominal moment  $M_{nc}$  when nonlinear behavior is developed. The elastic period of the structure is not altered with the definition and assignment of the Interaction PMM Hinge. The unloading behavior of the model from a yielded state follows the slope of the elastic stiffness of the structure, and permanent deformations are computed accordingly. The nonlinear behavior is defined through a normalized moment–rotation ( $M-\theta$ ) or moment–curvature ( $M-\phi$ ) relation with possible degrading behavior.

In this study, the concept of plastic rotation is considered for identifying the limit states. The real moment–rotation curve of a RC member in which the tension steel yields can be idealized to a simplified bilinear curve, as shown in Fig. 3 for a typical RC beam (Park and Paulay 1975). In Fig. 3, point B corresponds to the tensile yield strain in the steel indicating yield moment,  $M_y$ , and yield rotation,  $\theta_y$ , while point C corresponds to the ultimate conditions; namely ultimate moment,  $M_u$ , and corresponding ultimate rotation,  $\theta_u$ . The ultimate condition was considered to be the attainment of one of the following conditions; whichever happened first (Park and Paulay 1975; Ramin and Fereidoonfar 2015).

1. A 20% drop in the moment capacity of member.
2. When the tensile strain in the longitudinal steel reaches the ultimate tensile strain.
3. The attainment of the ultimate compression strain in concrete using the equation proposed by Scott et al. (1982).

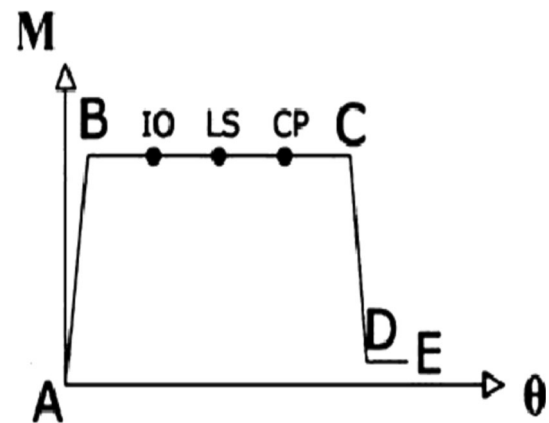


**Fig. 3** A typical real moment–rotation (or moment–curvature) and the corresponding idealized curve for a flexural plastic hinge

Although it is not the main focus of this study but the acceptance criteria of immediate occupancy (IO), life safety (LS) and collapse prevention (CP) were defined for the beam and columns similar to the ratios recommended in FEMA-356 (1997).

**Modeling soil nonlinearity**

Various methods have been developed for modeling soils surrounding a pile to be applicable in the Beam on Nonlinear Winkler Foundation method of analysis [Matlock (1970), Reese et al. (1974), Matlock et al. (1978), Nogami (1983), Makris and Gazetas (1992), Badoni and Makris (1995) and El-Naggar and Novak (1996)].

The general  $p-y$  model for sand as proposed by Reese et al. (1974) from the results of tests at Mustang Island on two 0.6 m diameter piles embedded in a deposit of

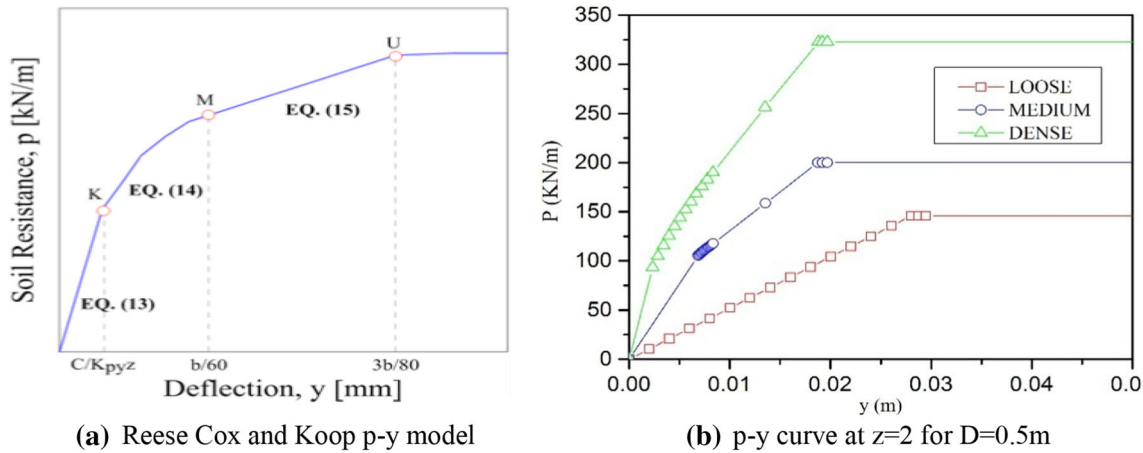


Fig. 4 *p*-*y* model for nonlinear Winkler spring

Table 1 Initial stiffness,  $K_{py}$  according to Reese et al. (1974)

	Loose ( $\varphi < 30^\circ$ )	Medium ( $30^\circ < \varphi < 36^\circ$ )	Dense ( $\varphi > 36^\circ$ )
$K_{py}$ (below water table) (MN/m <sup>3</sup> )	5.4	16.3	34
$K_{py}$ (above water table) (MN/m <sup>3</sup> )	6.8	24.4	61

submerged, dense, fine sand. The characteristic shape of the *p*-*y* curve is described by three straight line portions and a parabolic curve, as illustrated in Fig. 4.

The procedure is for short-term static loading. The ultimate soil resistance is given by the smallest results of the following two equations:

$$P_u = \gamma_z \left[ \frac{K_0 z \tan \varphi \sin \beta}{\tan(\beta - \varphi) \cos \alpha_s} + \frac{\tan \beta}{\tan(\beta - \varphi)} (b + z \tan \beta \tan \alpha_s) + K_0 z \tan \beta (\tan \varphi \sin \beta - \tan \alpha_s) - K_a b \right] \quad (1)$$

The *p*-*y* curve is composed by four parts: an initial straight line (2), a parabolic portion (3), and a final straight line (4):

$$P = K_{py} zy \quad (2)$$

with  $K_{py}$ , depending on  $f$  (Table 1).  $A_s$  and  $B_s$  are dimensionless parameters used in static loading and function of the depth and pile diameter.

$$P = C y^{1/n} \quad (3)$$

$$m = \frac{P_u - P_m}{y_u - y_m} n = \frac{P_m}{m y_m} C = \frac{P_m}{y_m^{1/n}} \quad (4)$$

$$P_{ms} = B_s P_u \quad (5)$$

$$P_{us} = A_s P_u \quad (6)$$

$$y = \frac{3b}{80}$$

The value of  $p$  remains constant after  $y = \frac{3b}{80}$ . Based on the *p*-*y* model described above, for example, Fig. 3b presents the *p*-*y* curve for  $z = 2$  m,  $D = 0.5$  m.

### Modeling soil–pile interaction

Pile–soil interaction phenomenon is modeled using nonlinear springs to account for local nonlinearities at the pile–soil interface. The nonlinear behavior of the soil is described by load transfer characteristics for both vertical and lateral soil reactions. Some other types of local nonlinearities such as slippage and gapping may occur at near surface soil–pile interface. To simplify the problem, the effect of gapping, slippage and settlement on the response of pile seems to be marginal in the case of lateral response analysis; only the lateral soil movement was analyzed in this paper.

The soil was modeled using nonlinear springs. The multi-linear plastic element available in SAP2000 (2002) was used in the proposed model. The nonlinear properties of link element were obtained using the generated *p*-*y* curve from 2D finite difference (FD) solution by LPILE. The springs were assigned at each 0.5 m along the pile. The *p*-*y* curves were developed in LPILE at the defined depth location and hence the soil stiffness at various depth locations was calculated and hysteretic behavior was obtained. The fixity was assigned at the bottom of the pile to simulate the embedment of the pile into rock.

### Performance-based methodology

The performance-based methodology necessitates the estimation of two quantities for assessment and design purposes. These are the seismic capacity and the seismic

demand. Seismic capacity means the ability of the building to resist the seismic effects. Seismic demand is a description of the earthquake effects on the building. The performance is evaluated in a manner such that the capacity is greater than the demand (ATC-40 1996). These quantities can be determined by performing either inelastic time-history analyses or nonlinear static ‘pushover’ analyses. The former is the most realistic analytical approach for assessing the performance of a structure, but it is usually very complex and time consuming mainly because of the complex nature of strong ground motions. This complexity has led to the adaptation of nonlinear static (NSA) analysis methods as necessary assessment and design tools. The most widely known NSA is the capacity spectrum method (CSM) or the displacement coefficient method (DCM). CSM is extensively employed compared to other NSP due to its visual and graphical nature, and its ability to provide rapid assessment of the relationship between capacity and demand curve. In common with other NSP, CSM is used to determine the displacement demand imposed on a structure which is expected to deform beyond its elastic range. Following the recommendation of CSM in ATC-40, the method was extensively investigated and various improvements were proposed.

As graphically presented in Fig. 5, the CSM requires the determination of three primary elements: capacity, demand and performance. The capacity spectrum can be obtained through the pushover analysis, which is generally produced based on the first mode response of the structure assuming that the fundamental mode of vibration is the predominant response of the structure. This pushover capacity curve approximates how a structure behaves beyond the elastic limit under seismic loadings. The demand spectrum curve

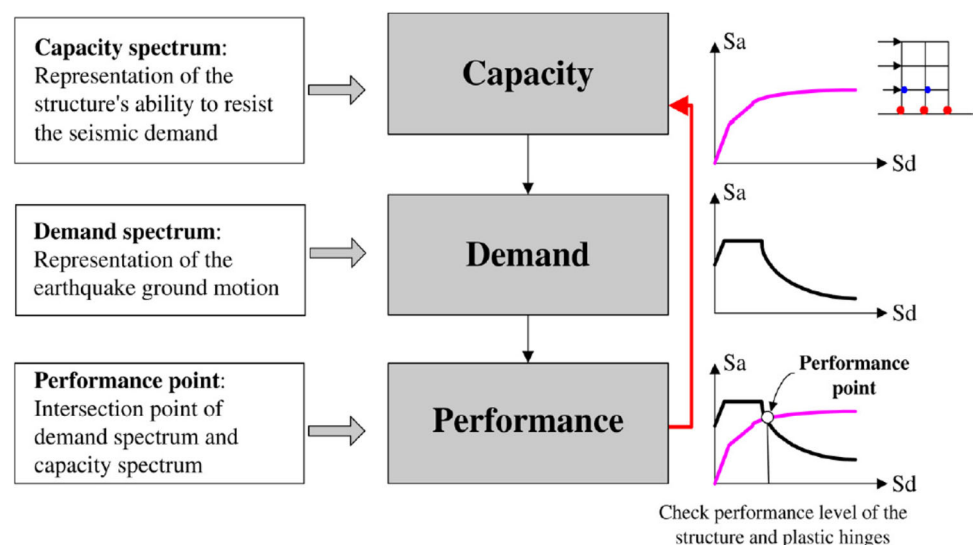
is normally estimated by reducing the standard elastic 5% damped design spectrum by the spectral reduction method. The intersection of the pushover capacity and demand spectrum curves defines the ‘‘performance point’’ as shown in Fig. 5. At the performance point, the resulting responses of the building should then be checked using certain acceptable criteria. The responses can be checked against acceptable limits on both global system levels (such as the lateral load stability and the inter story drift) and local element levels (such as the element strength and the sectional plastic rotation) (ATC-40 1996).

## Determination of limit states

Definition of limit states plays a significant role in the construction of the fragility curves. Limit states are of great importance since these values have a direct effect on the fragility curve parameters. This is especially true for special systems like soil–pile–structure for which the identification of limit states is highly dependent on the characteristics of the ISPS system.

The limit states used in this study are defined in terms of lateral drift since the behavior and the failure modes of such structures and pile are governed by deformation. To determine performance levels, the local limit states of members are obtained and then mapped into the capacity spectrum versus spectral displacement curve of the ISPS system. Local limit states are considered in terms of yield and ultimate curvatures. The performance levels of the most critical members are defined as the global limit states of the structure.

**Fig. 5** Capacity spectrum method



### Over-strength factors

Over-strength (Fig. 6) is a parameter used to quantify the difference between the required and the actual strength of a material, a component or a structural system. Structural over-strength is generally expressed by the ‘over strength factor’  $\Omega_d$  defined as follows:

$$\Omega_d = \frac{V_y}{V_d} \tag{7}$$

where  $V_y$  and  $V_d$  are the actual and the design lateral strengths of the system, respectively. The  $\Omega_d$ -factor is often termed as ‘observed over strength’ factor. The relationship between strength, over-strength and ductility is depicted in Fig. 6. For building structures, an additional measure relating the actual  $V_y$  to the elastic strength level  $V_e$  of lateral resisting systems has been suggested by Elnashai and Mwafy (2002) alongside the over-strength  $\Omega_d$  in Eq. (7). The proposed measure  $\Omega_i$  is given as:

$$\Omega_i = \frac{V_y}{V_e} \tag{8}$$

and is termed ‘inherent over-strength’ to distinguish it from the ‘observed over-strength’  $\Omega_d$  (Fig. 6) commonly used in the literature and suggested measure of response  $\Omega_i$  reflects the reserve strength and the anticipated behavior of the structure under the design earthquake, as depicted in Fig. 7. Clearly, in the case of  $\Omega_i \geq 1.0$ , the global response will be almost elastic under the design earthquake, reflecting the high over-strength of the structure. If  $\Omega_i < 1.0$ , the difference between the value of  $\Omega_i$  and unity is an indication of the ratio of the forces that are imposed on the structure in the post-elastic range. Structures with  $\Omega_i \geq 1.0$  should be treated with care since they may be redesigned to achieve substantial economies without jeopardizing safety.

### Ductility factors

Ductility is defined as the ability of a material, component, connection or structure to undergo inelastic deformations with acceptable stiffness and strength reduction or the capacity to dissipate energy. Figure 8 compares the structural response of brittle and ductile systems. In the figure, curves A and B express force–displacement relationships for systems with the same stiffness and strength but distinct post-peak (inelastic) behavior. Brittle systems fail after reaching their strength limit at very low inelastic deformations in a manner similar to curve A. The collapse of brittle systems occurs suddenly beyond the maximum resistance, denoted as  $V_{max}$ , because of lack of ductility. Conversely, curve B corresponds to large inelastic deformations, which are typical of ductile systems. Whereas the two response curves are identical up to the maximum resistance  $V_{max}$ , they should be treated differently under seismic loads. The ultimate deformations  $\delta_u$  corresponding to load level  $V_u$  are higher in curve B with respect to curve A, i.e.  $\delta_{u,b} \gg \delta_{u,A}$  (Elnashai and Di Sarno 2008).

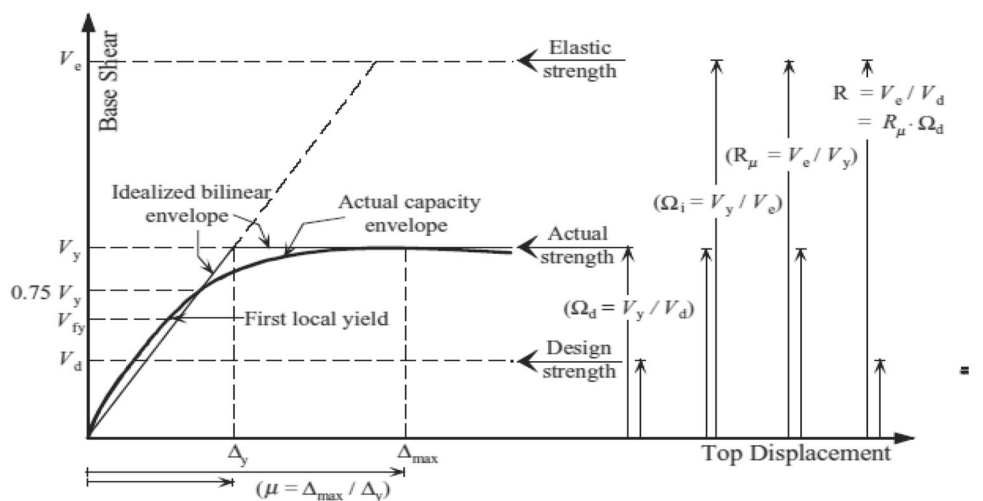
The structure ductility  $\mu$  is defined in terms of maximum structural drift ( $\delta_{max}$ ) and the displacement corresponding to the idealized yield strength ( $\delta_y$ ) as:

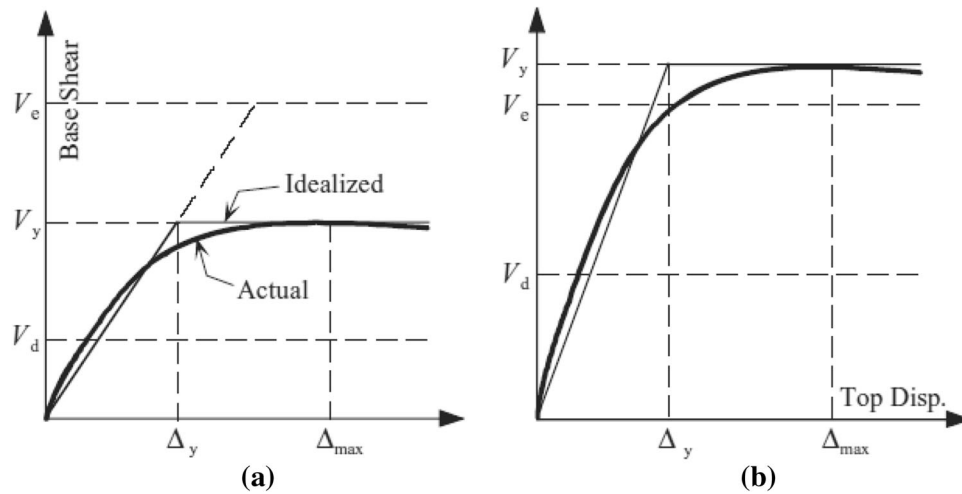
$$\mu = \frac{\delta_{max}}{\delta_y} \tag{9}$$

### Response modification factors

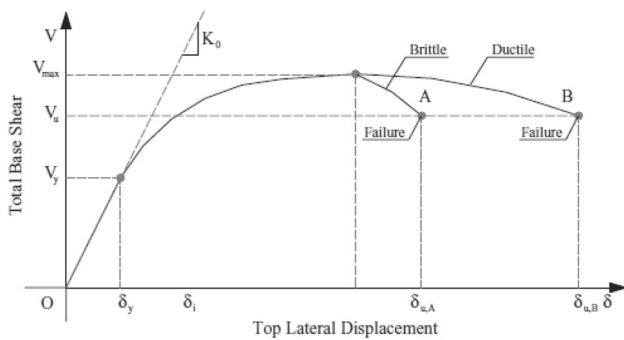
Mazzolani and Piluso (1996) addressed various theoretical approaches to compute the response modification factor ( $q_{factor}$ ), such as the maximum plastic deformation approach, the energy approach, and the low-cycle fatigue

Fig. 6 Relation between strength, over-strength and ductility





**Fig. 7** Different levels of inherent over-strength  $\Omega_i$ : ductile response,  $\Omega_i < 1.0$  (a), and elastic response under design earthquake  $\Omega_i \geq 1.0$  (b).  $V_d$  = design base shear strength;  $V_e$  = elastic base shear strength;  $V_y$  = actual base shear strength and  $\Delta$  = displacement



**Fig. 8** Definition of structure ductility

approach. ATC-19 proposed a simplified procedure to estimate the response modification factors, in which the response modification factor  $R$  is calculated as the product of the three parameters that profoundly influence the seismic response of structures:

$$R = R_0 R_\mu R_r \tag{10}$$

where  $R_0$  is the over-strength factor to account for the observation that the maximum lateral strength of a structure generally exceeds its design strength.

$R_\mu$  is a ductility factor which is a measure of the global nonlinear response of a structure, and  $R_r$  is a redundancy factor to quantify the improved reliability of seismic framing systems constructed with multiple lines of strength. In this study it is assumed that there are plenty of vertical lines of seismic framing system, and the redundancy factor is equal to 1.0. In this case the response modification factor is determined as the product of the over-strength factor and the ductility factor. Figure 9 represents the base-shear versus roof displacement relation of a structure, which can be developed by a nonlinear static

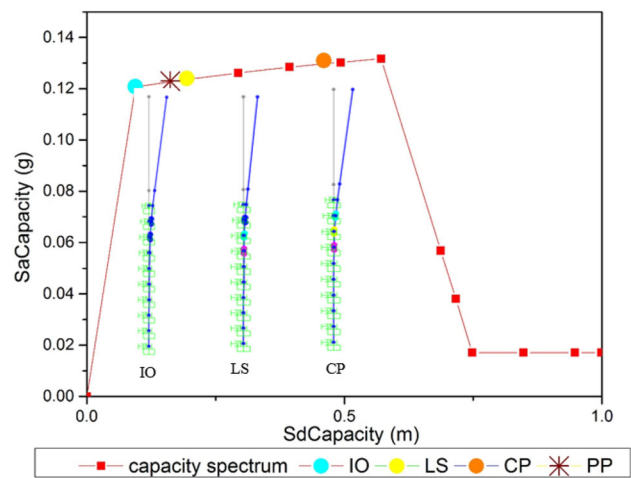


**Fig. 9** Typical performance curve for the ISPS

analysis. The ductility factor  $R_\mu$  and the over-strength factor  $R_0$  are defined as follows:

$$R_\mu = \frac{V_e}{V_y}, \quad R_0 = \frac{V_y}{V_d} \tag{11}$$

where  $V_d$  is the design base shear,  $V_e$  is the maximum seismic demand for elastic response, and  $V_y$  is the base shear corresponding to the maximum inelastic displacement.

### Validation model used in numerical study

The performance and ability of the proposed approach to simulate pile behavior in sand soil have been demonstrated by comparison between the numerical simulation and the test performed by Kampitsis et al. (2015). In these tests a

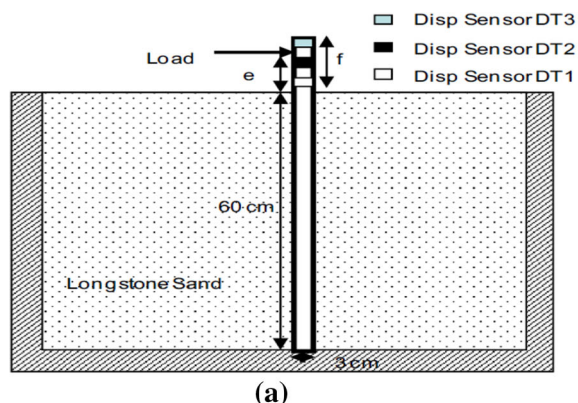
vertical pile is placed in a sand mass of uniform density. The dry unit weight and relative density of the specimen were measured to be  $\gamma_s = 16.2 \text{ KN/m}^3$  and  $D_r = 94\%$ , respectively. Laboratory results from tests sand indicated mean values of peak and critical-state angles of  $\varphi_p = 56$  at very small stress levels ( $< 10 \text{ kPa}$ ) and  $\varphi_{cv} = 32$ , respectively. The material and strength characteristics of the sand have been documented in Anastasopoulos et al. (2010).

The single pile was a hollow aluminum 6063-F25 cylinder of 3 cm external diameter, 2.8 cm internal diameter, and 60 cm length. The elasticity modulus of the pile is  $E_0 = 70 \text{ GPa}$  and the yield stress of the aluminum is 215 MPa. The pile was fixed at the base of the sandbox to ensure verticality during the sand running process. However, its length was sufficiently long for the bending failure (plastic hinge) not to be affected by the tip boundary conditions. The load is applied to the pile at a distance  $e = 32 \text{ cm}$  from ground surface. The experimental setup is portrayed in Fig. 10. For more details on the laboratory testing process the reader is referred to the studies of Gerolymos (2012) and Giannakos (2013).

In Fig. 11, the calculation of lateral force acting at 32 cm above the ground level with the corresponding displacement at the ground surface is obtained from the numerical model and compared with the resultant obtained from the experiment. It is observed that the tangent stiffness at low load level is over-estimated compared to the experimental result and the ultimate capacities are predicted precisely. One can deduce that the proposed numerical model can be employed providing a minimum calculation effort while retaining good precision for the obtained results for the soil–pile inelastic system.

## Parameters analysis

To evaluate the level of affecting parameters on the behavior of interaction soil–pile–structure, for this reason some parameters are adopted and are listed in Table 2;



## Geometry model

The structure studied in this paper is a bridge constructed in Algeria, as illustrated in Fig. 12. The single-column is 3 m high above the ground and extends to a depth of 5 m below the ground with uniform dimensions and reinforcement details. It carries a total weight of 500 kN that is assumed to act at a superstructure mid height of 3 m above ground level. The model includes nonlinear  $p$ – $y$  soil springs at different depths as shown in Fig. 12. The nonlinear  $p$ – $y$  soil spring elements used in the model are based on a NL-multi-linear plastic. The design criteria for selecting beam and column dimensions are corresponding to linear static analysis. The longitudinal and transverse reinforcements, characteristic and dimensions of the model are assigned according to Table 3. The assigned plastic hinges at capable plastic points and the acceptance criteria of rotation and translation displacement are defined in Table 3.

## Earthquake ground motions

The accelerograms used in this investigation are the horizontal components of the NORTHRIDGE, NEWHALL, NORICIA ITALY earthquakes records, Figs. 13 and 14. These records are believed to be representative of strong earthquake. Studies by Clough and Benuska (1966) indicate that structural response depends primarily on the peak acceleration impulse in the ground motion and that continuing motions of smaller amplitude have only a small effect on the maximum response. The peak ground acceleration of the horizontal component of NORTHRIDGE is 0.57 g, that of NEWHALL is 0.578 g and that of NORICIA ITALY is 0.521 g (Figs. 13, 14). Figure 15 show the elastic Acceleration response specter for the Northridge ground motion, NEWALL and NORICIA ITALY earthquakes records.

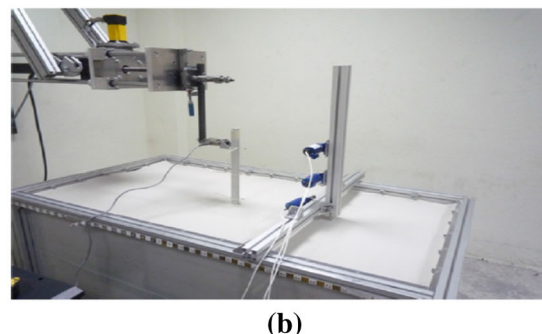
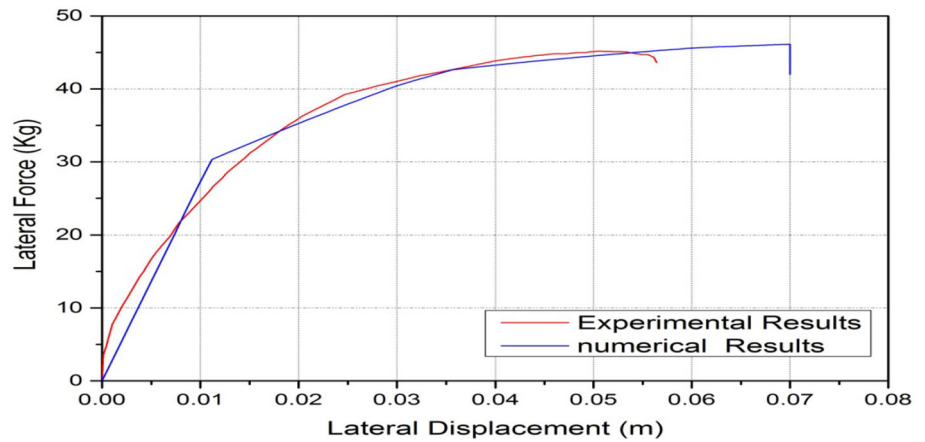


Fig. 10 Pushover model setup; geometry (a) and instrumentation (b)



**Fig. 11** Experimental and numerical force–displacement curves at pile head



**Table 2** Parametric cases

Parameter	Value
Axial force, $P/(f_c \cdot A_g)$	0, 0.1, 0.2, 0.3
Pile diameter, $D$ (m)	0.5, 0.7, 1, 1.2 m
Longitudinal steel ratio	3, 4, 5, 6%
Length of pile $L$ (m)	5, 7, 10
Type of soil	Loose, medium, dense

## Results and discussions

### Effects of axial load

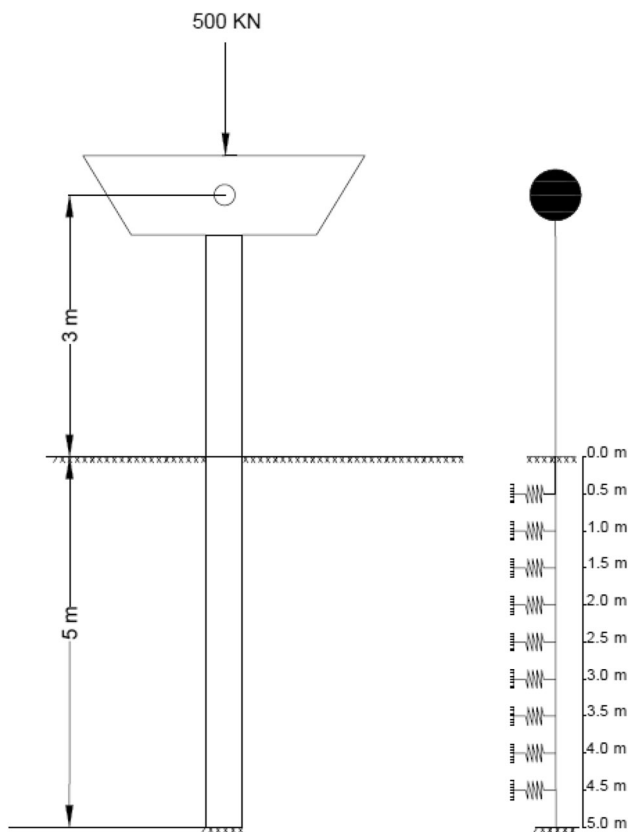
Piles are commonly used to transfer vertical forces, arising primarily from super structure. But for some structures, the primary function of pile is to transfer the lateral loads to soil. In many places in addition with the vertical forces, piles are also transferring the lateral forces due to heavy wind, earthquakes, slope failure, and lateral spread induced by liquefaction of soil.

According to current day practice, piles are independently analyzed first for the vertical load to determine their bearing capacity and settlement and then for the lateral load to determine the flexural behavior, This approach is valid only for small lateral loads, however, in case of coastal/offshore applications, the lateral loads are significantly high of the order of 10–20% of the vertical loads and in such cases, studying the interaction effects due to combined vertical and lateral loads is essential, which calls for a systematic analysis.

Figures 16a, 17a and 18a shows Lateral load–displacement response for the ISPS system, and Figs. 16b, 17b and 18b present the capacity spectrum versus spectral displacement curve, limit state and final performance point behavior for the ISPS system in loose, medium and dense sand under the influence of the axial load, respectively.

The lateral response in the fixed systems is greater than the lateral response of ISPS system with levels of axial load equals to 0.1 in loose sand, but in another case, the response of fixed system is lower than ISPS system and the initial stiffness is the same in all cases. Because when increase in level of density (loose, medium and dense) of sand gives highest vertical soil stresses which develop in the sand along the pile surface leading to higher lateral stresses in sand.

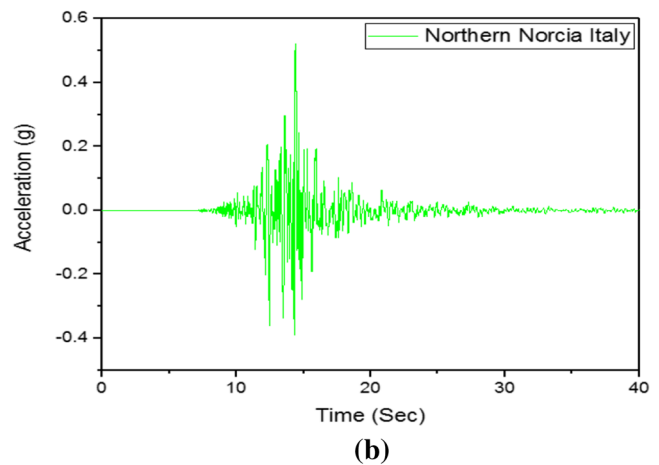
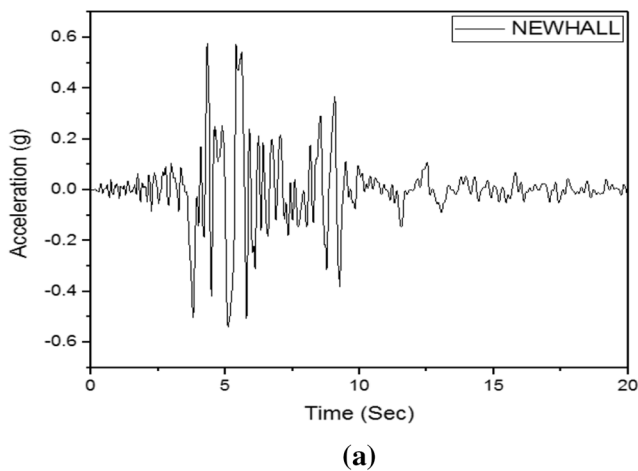
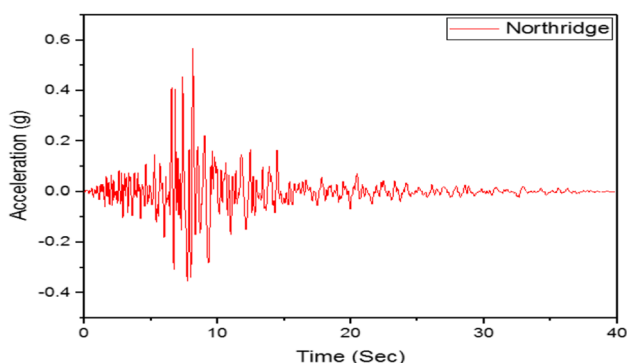
It is seen from these figures that in loose, medium and dense sand, the lateral capacity increases in the ISPS



**Fig. 12** Interaction soil–pile–structure configuration

**Table 3** Dimensions of pile and column and acceptance criteria of rotation and translation displacement

Components	Dimensions of circular section ( $D$ )	Bars and stirrups	Hinges	Moment plastic	Acceptance criteria					
					B	IO	LS	CP	D	E
Column	0.5 m	23 $\phi$ 16 $\phi$ 10@10 cm	Flexural + axial (P + M3)		0.005	0.012	0.015	0.015	0.025	
Pile	0.5 m	20 $\phi$ 20 $\phi$ 10@10 cm	Flexural (M3)	486.57	0	0.005	0.015	0.02	0.02	0.03
	0.7 m	20 $\phi$ 20 $\phi$ 10@10 cm	Flexural (M3)	766.93	0	0.005	0.015	0.02	0.02	0.03
	1	20 $\phi$ 20 $\phi$ 10@10 cm	Flexural (M3)	1172.0	0	0.005	0.015	0.02	0.02	0.03
	1.2	20 $\phi$ 20 $\phi$ 10@10 cm	Flexural (M3)	1437.8	0	0.005	0.015	0.02	0.02	0.03
	0.5	26 $\phi$ 20 $\phi$ 10@10 cm	Flexural (M3)	607.9	0	0.005	0.015	0.02	0.02	0.03
	0.5	33 $\phi$ 20 $\phi$ 10@10 cm	Flexural (M3)	771.5	0	0.005	0.015	0.02	0.02	0.03
	0.5	39 $\phi$ 20 $\phi$ 10@10 cm	Flexural (M3)	911.8	0	0.005	0.015	0.02	0.02	0.03

**Fig. 13** **a** NEWALL earthquake record, **b** NORICIA ITALY earthquake record**Fig. 14** Northridge earthquake record

system in the range of 12.5–5.3% when increase in level of axial load, it is clear that the lateral capacities of the ISPS system in sands improve in general under the presence of axial loads. This could be attributed to the pile and column sections in ISPS system subjected to higher axial force level with great sectional stiffness and yield moment.

Figures 16b, 17b and 18b show that, when increasing axial load the spectral acceleration decreases because the mass and the period of ISPS system are increasing in all cases.

The performance point (PP) to be located between the LS–CP for axial load of level 0.1, for levels 0.2 and 0.3 it is

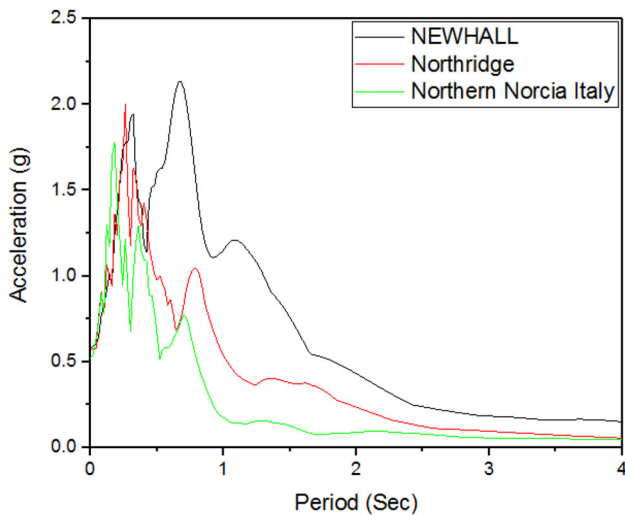


**Fig. 15** Elastic acceleration response spectra of Northridge, NEWHALL and NORICIA ITALY earthquakes records

located in IO–LS for Northridge earthquake. For NORICIA ITALY earthquake the PP is located before IO, and for NEWHALL earthquake, it is located between LS–CP.

Figures 16c, 17c and 18c show the formations of plastic hinges, which are affected by the type of sand and the variation in axial load. For the cases of loose sand the plastic hinge is formed in the base of the column and not affected by increasing axial load. Because the loose sand gives more deflection in the pile and this deflection is not supported by columns.

And in the cases of the medium and dense sand, the plastic hinge appears in the base of the column for axial load equals to 0, 0.1, and formed at 1 m under the head of the pile for axial load equal to 0.2, 0.3. Because the level of axial load gives a higher sectional stiffness and yield moment for the column.

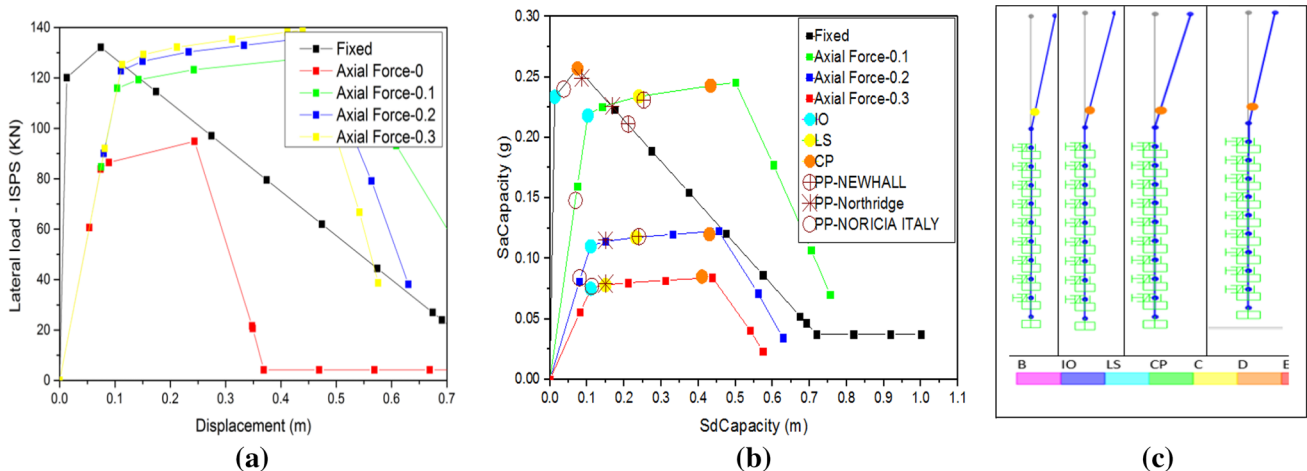


**Fig. 16** a Lateral load–displacement behavior ISPS, b performance curve for the ISPS, c formation of plastic hinge, in loose sand under the influence of the axial load

From response modification factors presented in Fig. 19c, it can be observed that the response modification factors decrease as the axial load level increases in ISPS system for all types of sand.

Figure 19b shows the ductility factor, it can be seen that for loose and medium sand the ductility is increasing for different axial load level in ISPS system. And for dense sand the ductility is decreased in ISPS system when the axial load increases.

The over-strength factors are plotted in Fig. 19a, it can be observed that the over-strength factors of ISPS system is not affected by increased axial load level by changing the type of sand.

**Effects of the section of pile**

Figures 20, 21 and 22 illustrate the pushover curves of ISPS system, the capacity spectrum of ISPS and the positions of plastic hinge, which are the same axial level load, steel ratio, different soils, and pile diameter of 0.5, 0.7, 1, 1.2 m, respectively.

As noted, the lateral capacity in ISPS system is increasing with increasing pile diameter, and not affected by soil type. For the reason that large pile diameter gives high strength in the pile this leads to high value in the lateral capacity.

Figures 20b, 21b and 22b show that, with increase in pile diameter, the spectral acceleration increase because of the rigidity of the ISPS system is increasing and period is decreasing. The performance point (PP) is located between IO–CP for all cases of earthquake.

Figures 20c, 21c and 22c displays the positions of plastic hinge, the plastic hinge are formed in more case at the column. Because the pile is height strength to the column.

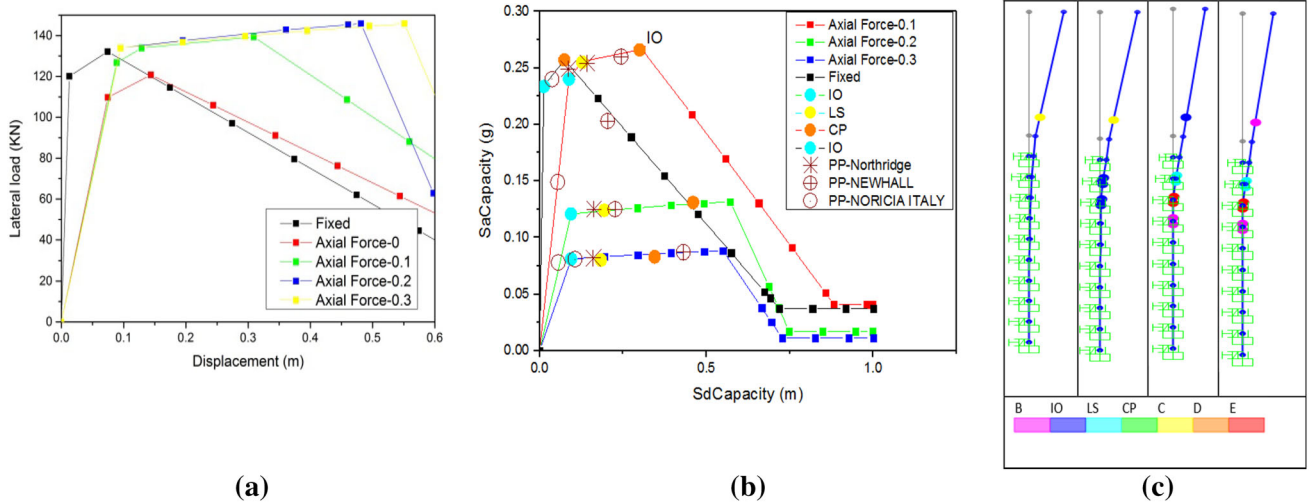


**Fig. 17** a Lateral load–displacement behavior ISPS, b performance curve for the ISPS, c formation of plastic hinge, in medium sand under the influence of the axial load

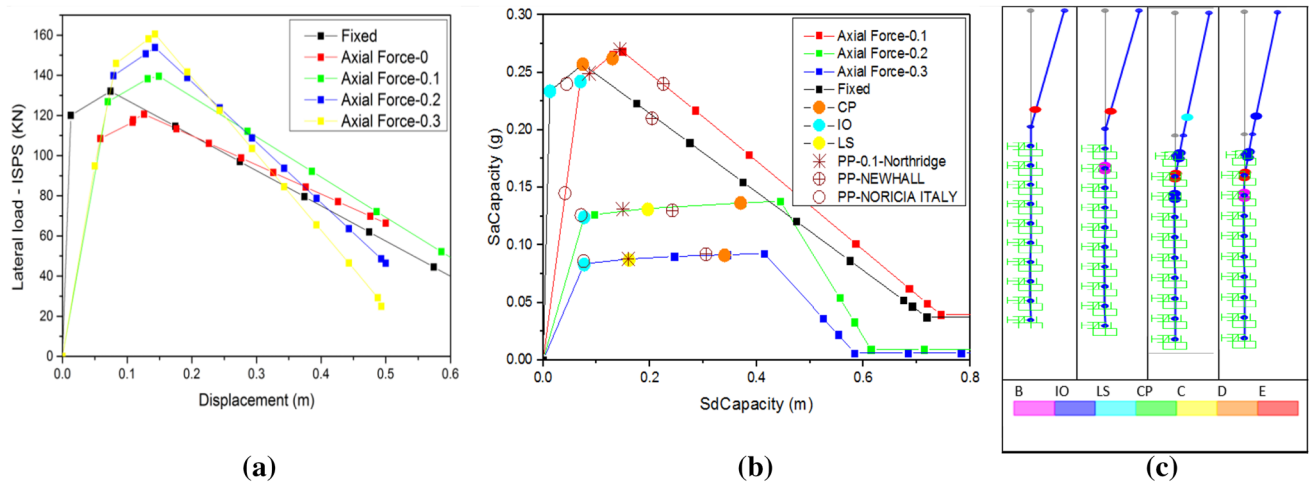


**Fig. 18** a Lateral load–displacement behavior ISPS, b performance curve for the ISPS, c formation of plastic hinge, in dense sand under the influence of the axial load

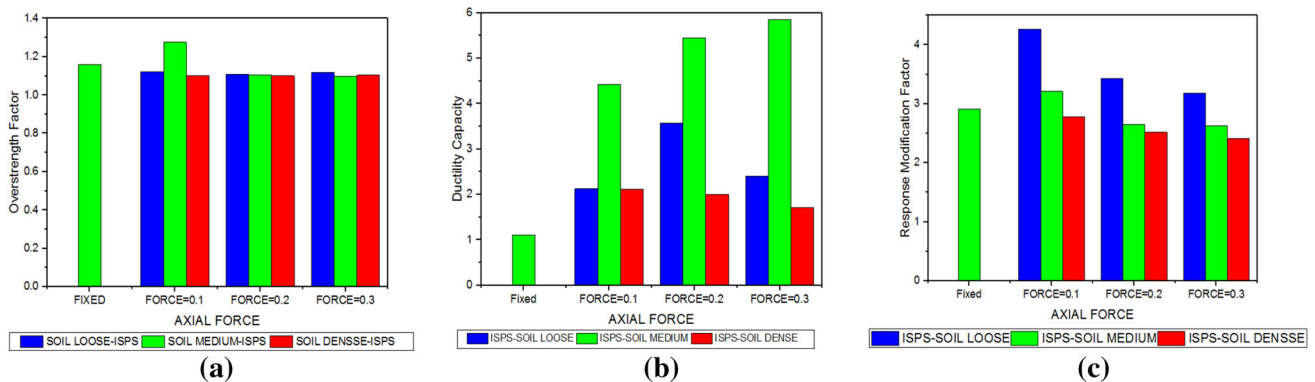


**Fig. 19** a Over-strength factor, b ductility and c the response modification factors for ISPS and ISP system under the influence of the axial load

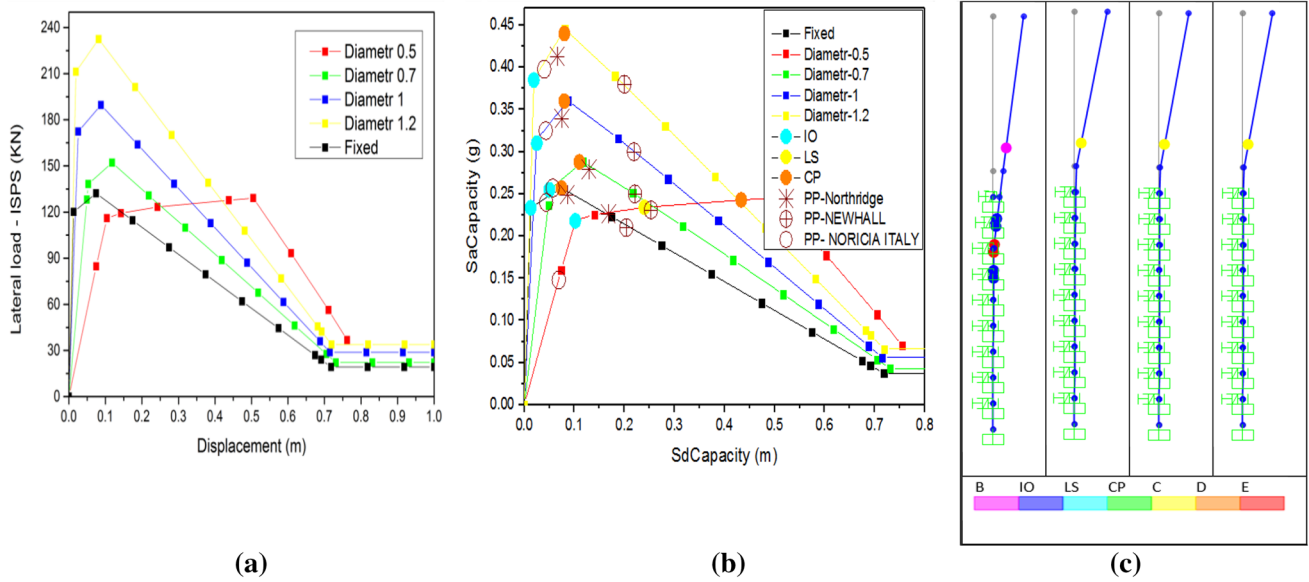


**Fig. 20** a Lateral load–displacement behavior ISPS, b performance curve for the ISPS, c formation of plastic hinge, in loose sand under the influence of the section of pile

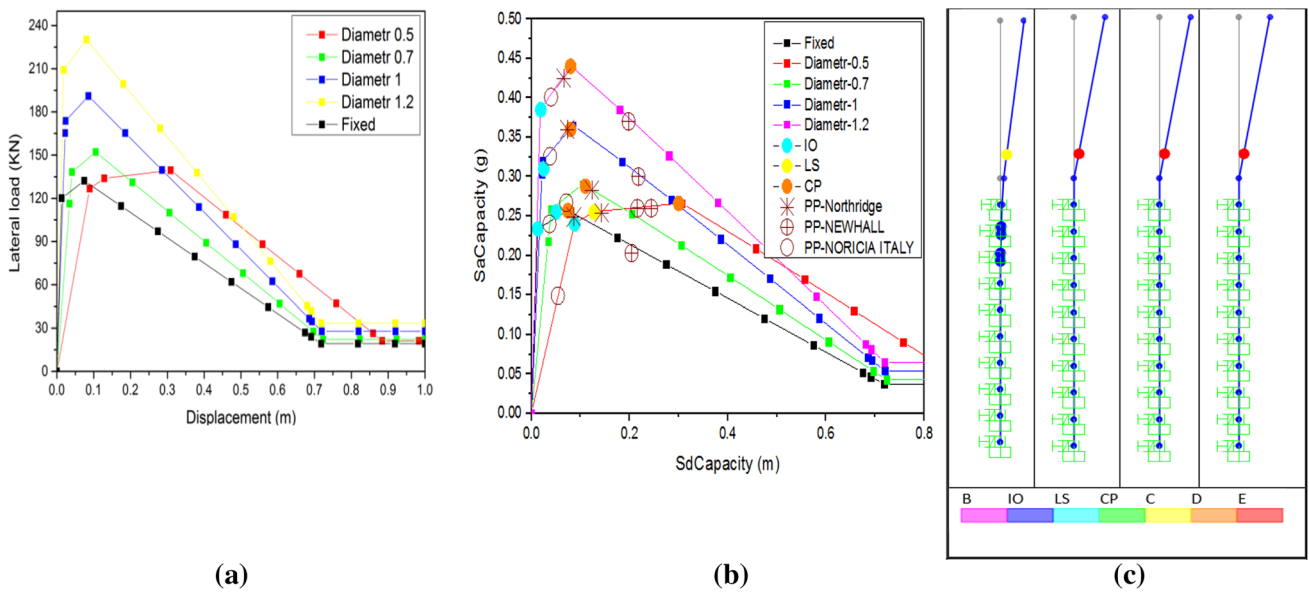


**Fig. 21** a Lateral load–displacement behavior ISPS, b performance curve for the ISPS, c formation of plastic hinge, in medium sand under the influence of the section of pile

Figure 23 presented the over-strength factor, ductility and the response modification factors for ISPS system under the influence of pile diameter. The increasing pile diameter leads to an increase in the lateral capacity of the pile, but the over-strength was not affected in the ISPS system compared with the fixed system.

In loose sand, the ductility increases for diameters 0.5, 0.7 m with 57.14, 71.4% and decreases for 1, 1.2 m with 8, 19% compared with the fixed system. For medium and dense sand, the ductility is decreased in all different cases of the pile diameter.

In all sand types (loose, medium, dense) the response modification factor ( $R$ ) is decreasing in the ISPS system with increasing pile diameter.

### Effects of longitudinal steel ratio

Figures 24, 25 and 26 illustrate the lateral capacity for the ISPS system under the effect of longitudinal steel ratio ( $A_s = 3, 4, 5, 6\%$ ) with different sand types (loose, medium, dense).

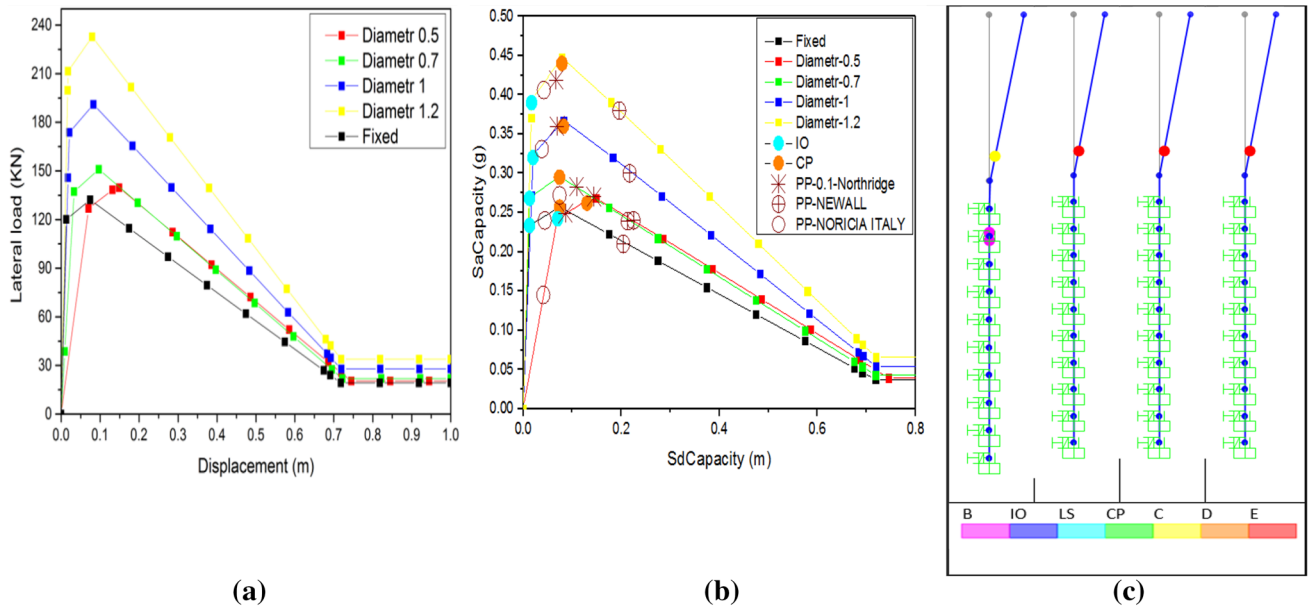


**Fig. 22** a Lateral load–displacement behavior ISPS, b performance curve for the ISPS, c formation of plastic hinge, in dense sand under the influence of the section of pile

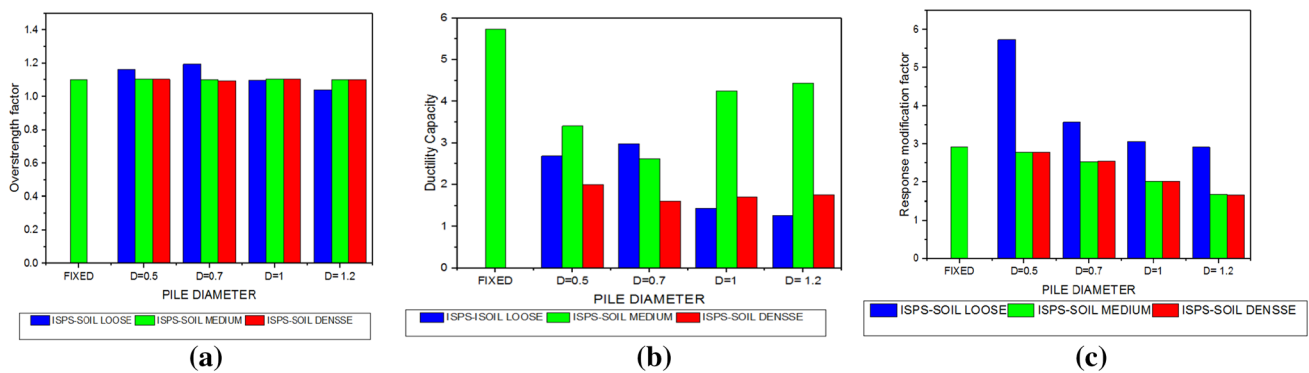


**Fig. 23** a Over-strength factor, b ductility and c the response modification factors for ISPS and ISP system under the influence of pile diameter

For all sand types, in the ISPS system the lateral capacity is not affected by the increasing longitudinal steel ratio in pile for medium, dense sand and in loose sand when  $A_s = 4, 5$  and  $6\%$ .

With increasing longitudinal steel ratio, the spectral acceleration is not affected because the characteristics dynamic do not change in ISPS system. And the performance point (PP) is located between LS and CP in almost all cases.

For loose and medium sand the position of plastic hinges are formed in pile for cases of ( $A_s$ ) equal to  $3\%$ , but in dense sand and other cases for loose and medium sand the plastic hinges are formed in the base of column.

Figure 27 illustrates the over-strength factor, ductility and the response modification factors for ISPS system under longitudinal steel ratio.

For loose sand, the response modification factor ( $R$ ) is decreasing in ISPS system when increase in the longitudinal steel ratio. In medium and dense, the  $R$  is not affected.

The ductility in all types of sand is low when compared to fixed systems, and when increase in the value of longitudinal steel ratio ( $A_s$ ) the ductility is decrease in ISPS system. The over-strength is not affected by increase in longitudinal steel ratio.

### Effects of length of pile

Figures 28a, 29a and 30a show the lateral capacity in the ISPS system under the influence of the length of pile ( $L = 5, 7.5, 10$  m) with different sand types (loose, medium, dense). For all sand types, when increase in the length of pile the lateral capacity increase slightly. Because of the

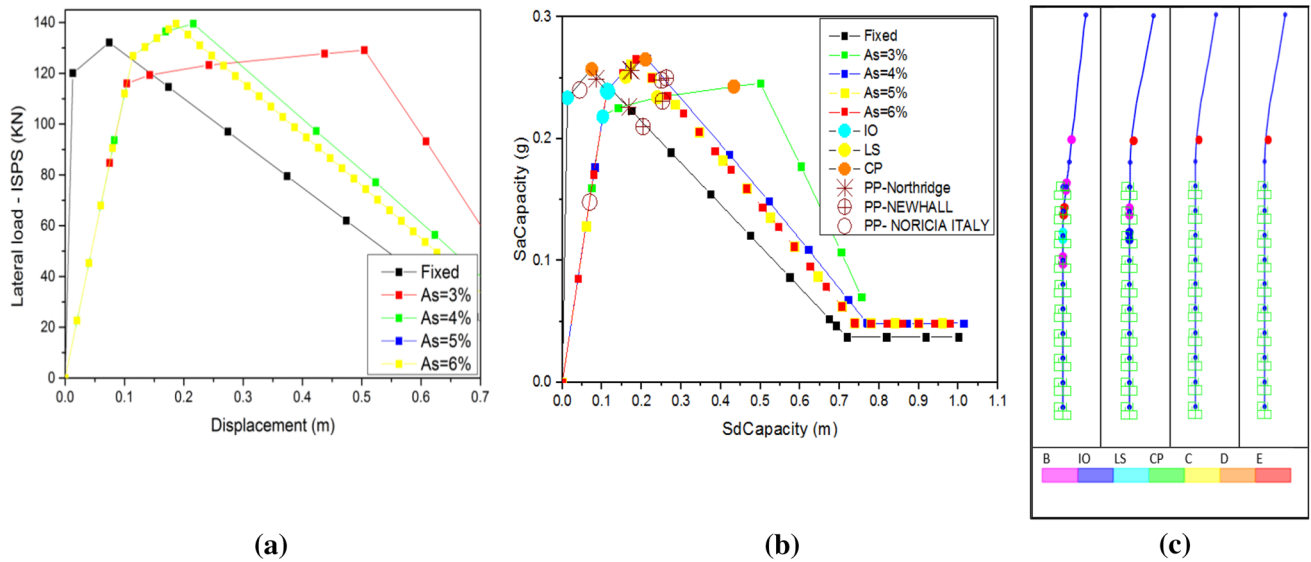


**Fig. 24** a Lateral load–displacement behavior ISPS, b performance curve for the ISPS, c formation of plastic hinge, in loose sand under the influence of longitudinal steel ratio

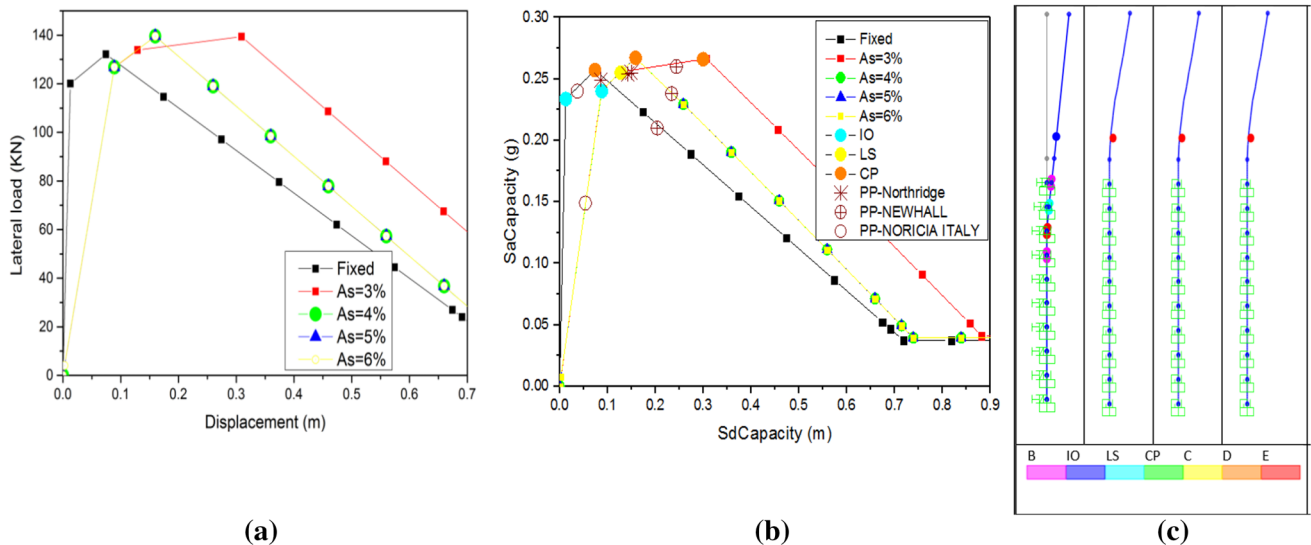


**Fig. 25** a Lateral load–displacement behavior ISPS, b performance curve for the ISPS, c formation of plastic hinge, in medium sand under the influence of longitudinal steel ratio

augmentation in length of pile drive to more fixing in the sand, this leads to more stabilization in ISPS system.

Figures 28b, 29b and 30b show that, with increase in length of pile, the spectral acceleration increases slightly. And the performance point (PP) is located after CP in Newhall and Northridge but for NORICIA ITALY the PP is located before IO.

Figure 28c, 29c and 30c show, for loose sand the position of plastic hinge is affected by the length of pile and is formed at the top of the pile. The plastic hinge in case of medium sand is formed at the top of pile in case of pile 5 m and for the other cases the plastic hinge is formed at the

base of column. In the case of dense sand, the position of plastic hinge is not affected and it appears at the base of column.

Figure 31 presents the over-strength factor, ductility and the response modification factors for ISPS system with variation in length of pile.

The over-strength factors are not affected by increasing the length of the pile. The ductility in loose sand is increased, for medium sand is decreasing and in dense sand is not affected by increases in length of the pile.

The value of response modification factors (*R*) is greater to fixed case and decrease when increase in length of the

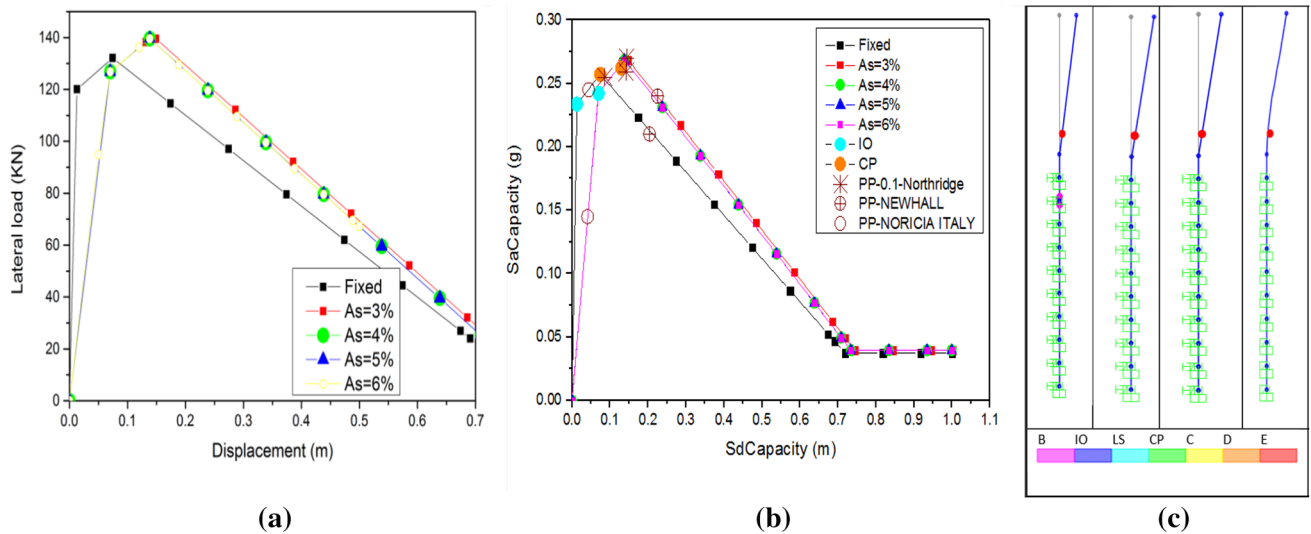


**Fig. 26** a Lateral load–displacement behavior ISPS, b performance curve for the ISPS, c formation of plastic hinge, in dense sand under the influence of longitudinal steel ratio

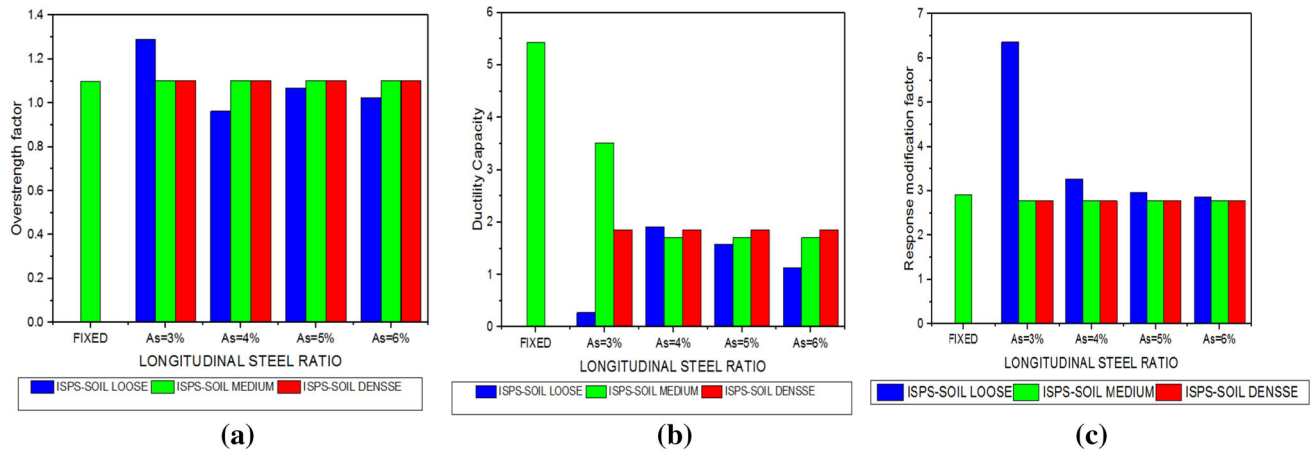


**Fig. 27** a Over-strength factor, b ductility and c the response modification factors for ISPS and ISP system under the influence of longitudinal steel ratio

pile in loose sand, and not affected in the medium and dense sand.

### Conclusion

A static nonlinear analysis of the response of soil–pile–structure interaction behavior of a single laterally loaded pile in sand deposits was investigated using a finite element (FE) model based on a beam-on-nonlinear-Winkler (BNWF) approach. The following conclusion can be made related to the influence of the axial force, pile diameter, longitudinal steel ratio, length of pile, and type of soil:

- In most of the cases, the lateral capacity of fixed system is low compared to lateral capacity in ISPS system when increasing the axial load, pile diameter, longitudinal steel ratio, and length of pile in all types of sand.
- The augmentation in axial load leads to a slight increase in ISPS system for loose, medium and dense sand. The spectral acceleration decrease in all cases. The performance points (PP) is affected by types of sand, axial load and frequency content earthquake record.
- The augmentation in pile diameter, leads to increase in lateral capacity and spectral acceleration in ISPS system. The position of PP is not affected by the augmentation in pile diameter.



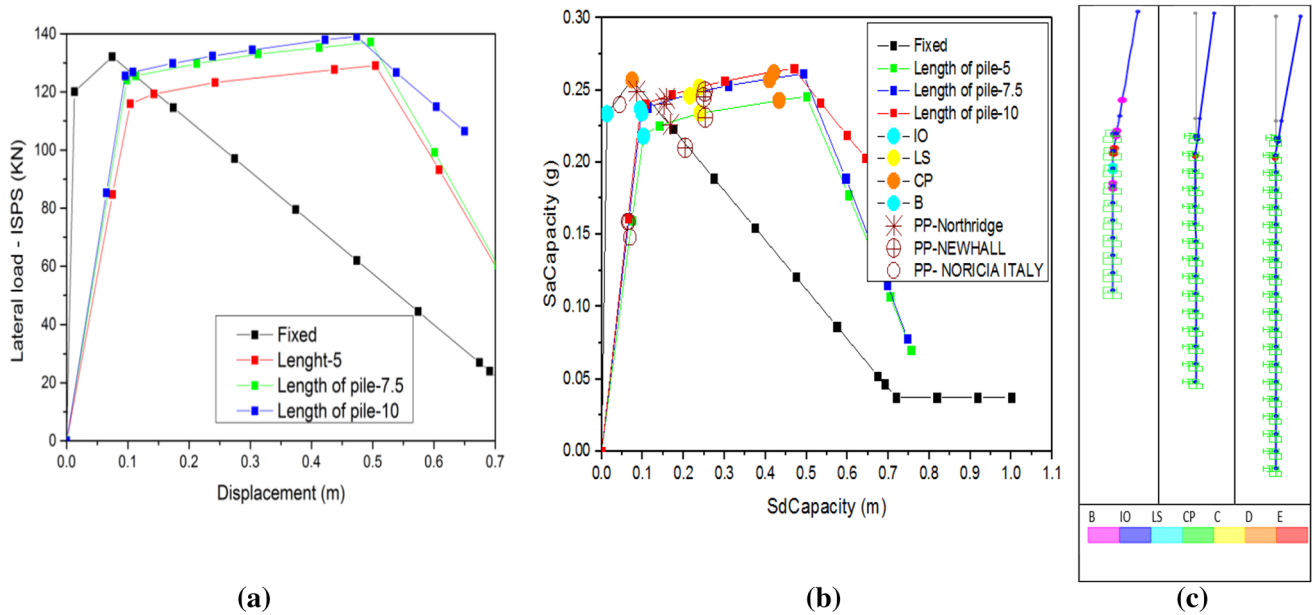


**Fig. 28** a Lateral load–displacement behavior ISPS, b performance curve for the ISPS, c formation of plastic hinge, in loose sand under the influence of length of pile

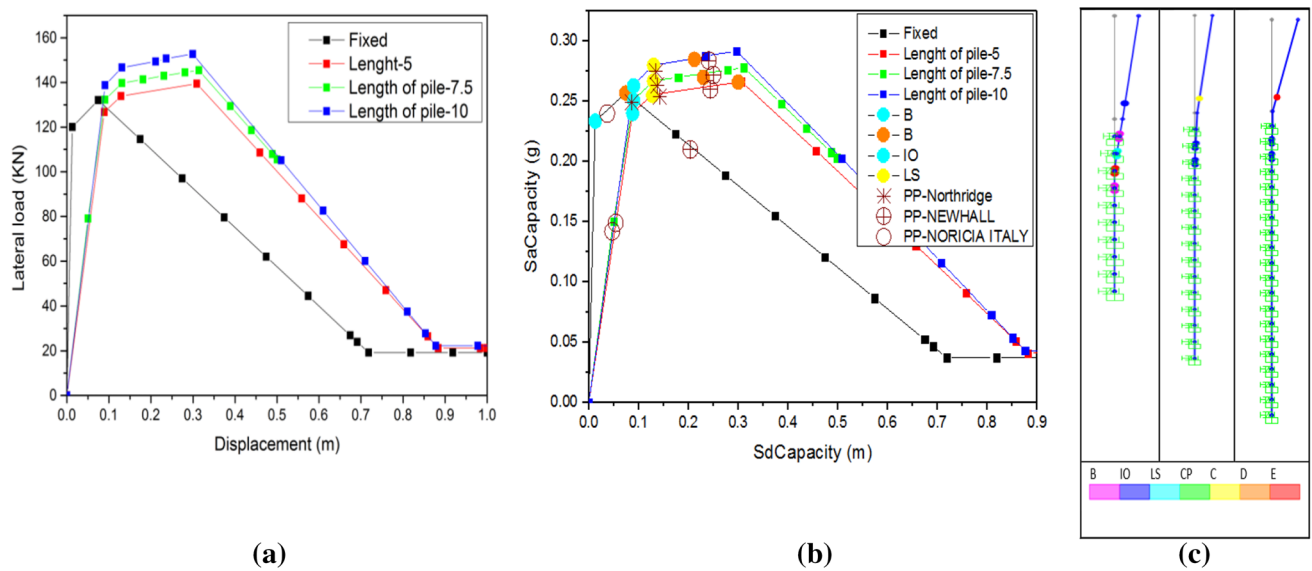


**Fig. 29** a Lateral load–displacement behavior ISPS, b performance curve for the ISPS, c formation of plastic hinge, in medium sand under the influence of length of pile

- The lateral capacity and spectral acceleration are not affected by the augmentation in longitudinal steel ratio.
- The influence of length of pile is less significant for lateral capacity and specter accelerations, the performance points (PP) are not affected.
- The formation and the position of plastic hinges are affected by the type of sand, axial load level, pile diameter, longitudinal steel ratio, and length of pile.
- The over-strength factor is not affected when increasing the axial load level, pile diameter, and length of pile, but decreases with increasing longitudinal steel ratio.

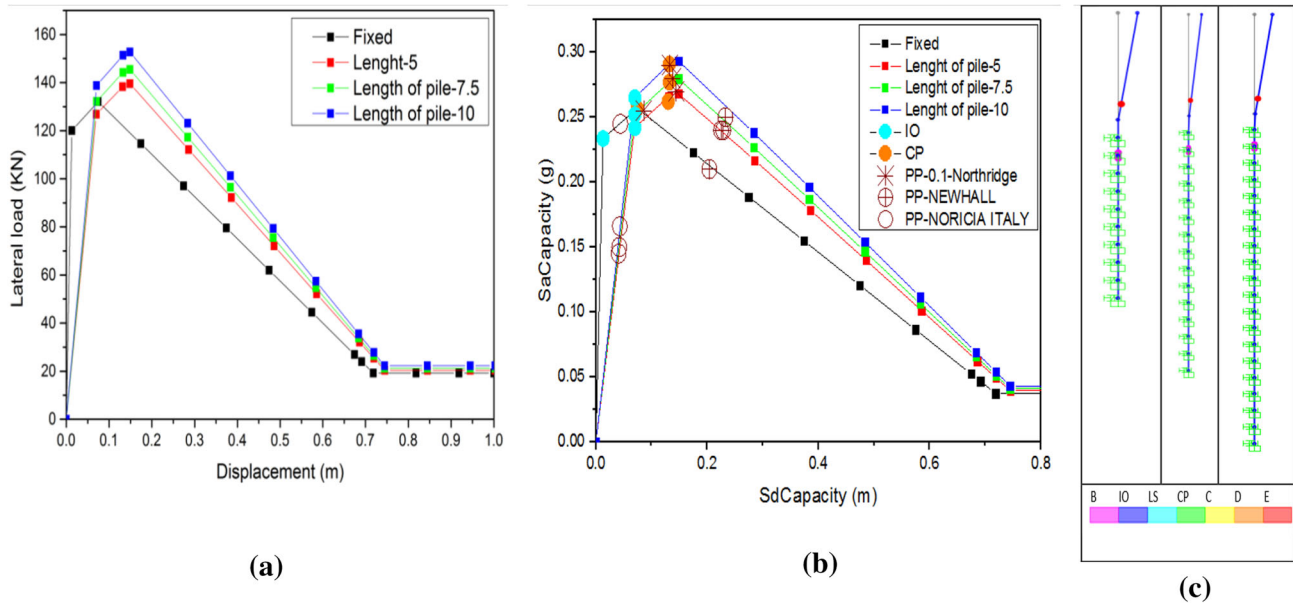


Fig. 30 a Lateral load–displacement behavior ISPS, b performance curve for the ISPS, c formation of plastic hinge, in dense sand under the influence of length of pile

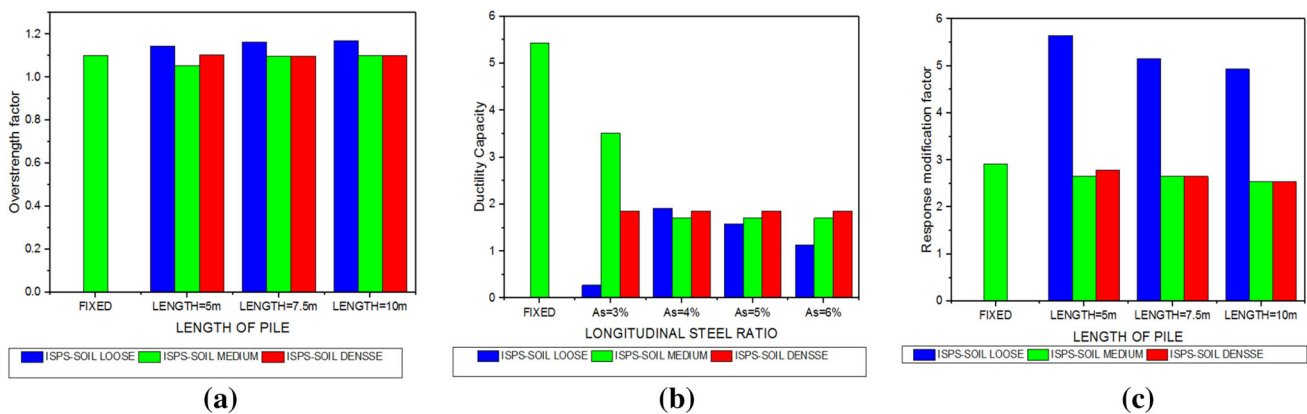


Fig. 31 a Over-strength factor, b ductility and c the response modification factors for ISPS and ISP system under the influence of pile length

- The response modification factor ( $R$ ) and ductility are affected by increasing axial load level, pile diameter, length of pile and longitudinal steel ratio.

### References

Anastasopoulos, I., Georgarakos, P., Georgiannou, V., Drosos, V., & Kourkoulis, R. (2010). Seismic performance of bar-mat reinforced-soil retaining wall: shaking table testing versus numerical analysis with modified kinematic hardening constitutive model. *Soil Dynamics and Earthquake Engineering*, 30, 1089–1105.

ATC. (1996). *Seismic evaluation and retrofit of concrete buildings—volume 1 (ATC-40)*. Report No. SSC 96-01. Redwood City: Applied Technology Council.

Badoni, D. & Makris, N. (1995). Nonlinear response of single piles under lateral inertial and seismic loads. *Soil Dynamics and Earthquake Engineering*, 15, 29–43.

Chiou, J. S., and Chen, C. H. (2010). Displacement ductility capacity of fixed-head piles. *Proceedings of 5th International Conference on Recent Advance in Geotechnical Earthquake Engineering and Soil Dynamics*, Missouri University of Science and Technology, Rolla, MO, Paper No. 9–10.

Chiou, J. S., Tsai, Y. C., & Chen, C. H. (2012). Investigating influencing factors of the ductility capacity of a fixed-head reinforced concrete pile in homogeneous clay. *Journal of Mechanics*, 28(3), 489–498.

Chiou, J. S., Yang, H. H., & Chen, C. H. (2009). Use of plastic hinge model in nonlinear pushover analysis of a pile. *Journal of Geotechnical and Geoenvironmental Engineering*, 135(9), 1341–1346.

Clough, R. W., Bensuka, K. L., & Lin, T. Y. (1966). *FHA, Study of Seismic Design Criteria for High Rise Building*, Washington D.C.U.S, Federal Housing Administration, HUD TS-3.

- Elnashai, A. S., & Mwafy, A. M. (2002). Calibration of force reduction factors of RC buildings. *Journal of Earthquake Engineering*, 6(2), 239–273.
- Elnashai, A. S., & Di Sarno, L. (2008). *Fundamentals of Earthquake Engineering*. New Jersey: Wiley.
- El-Naggar M. H., Novak, M. (1996). Nonlinear analysis for dynamic lateral pile response. *Soil Dynamics and Earthquake Engineering*, 15(4), 223–244.
- FEMA-356. (1997). Prestandard and commentary for the seismic rehabilitation of buildings. Washington, DC.
- Gerolymos, N. (2012). A macro-element model for nonlinear static and dynamic response of piles. Technical report for PEVE 2008 research project (contract number 65/1694). Laboratory of Soil Mechanics, NTUA.
- Giannakos, S. (2013). Contribution to the static and dynamic lateral response of piles (Doctoral dissertation, National Technical University of Athens, 2013).
- Guin, J., & Banerjee, P. K. (1998). Coupled soil–pile–structure interaction analysis under seismic excitation. *Journal of the Structural Engineering. American Society of Civil Engineers*, 124, 434–444.
- Hussien, M. N., Tobita, T., Iai, S., & Rollins, K. M. (2012). Vertical load effect on the lateral pile group resistance 522 in sand response. *International Journal of Geomechanics and Geoengineering*, 7(4), 263–282.
- Kampitsis, A. E., Giannakos, S., Gerolymos, N., & Sapountzakis, E. J. (2015). Soil–pile interaction considering structural yielding: Numerical modeling and experimental validation. *Engineering Structures*, 99, 319–333.
- Karthigeyan, S., Ramakrishna, V. V. G. S. T., & Rajagopal, K. (2006). Influence of vertical load on the lateral response of piles in sand. *Computers and Geotechnics*, 33(2), 121–131.
- Karthigeyan, S., Ramakrishna, V. V. G. S. T., & Rajagopal, K. (2007). Numerical investigation of the effect of vertical load on the lateral response of piles. *Journal of Geotechnical and Geoenvironmental Engineering*, 133(5), 512–521.
- Khodair, Y., & Abdel-Mohti, A. (2014). Numerical analysis of soil–pile interaction under axial and lateral loads. *International Journal of Concrete Structures and Materials*, 8(3), 239–249.
- Makris, N. & Gazetas, G. (1992). Dynamic Pile-Soil- Pile Interaction Part II. Lateral and Seismic Response. *Earthquake Engineering & Structural Dynamics*, 21(2), 145–162.
- Matlock, H. (1970). Correlations for Design of Laterally Loaded Piles in Soft Clay. Presented at the Second Annual Offshore Technology Conference, Houston, Texas, Vol 1, pp 577–588.
- Matlock, H., Foo, S. H. C., Bryant, L. M. (1978). Simulation of lateral pile behavior under earthquake motion. *Proceedings of the Specialty Conference on Earthquake Engineering and Soil Dynamics. ASCE* (pp. 600–619) Pasadena.
- Mazzolani, F. M., & Piluso, V. (1996). *Theory and design of seismic resistant steel frames*. Spon: E & FN.
- Nogami, T. (1983). Dynamic group effect in axial responses of grouped piles. *Journal of Geotechnical Engineering Division, ASCE*, 109(2), 228–243.
- Park, R., & Paulay, T. (1975). *Reinforced concrete structures*. NY: Wiley.
- Ramin, K., & Fereidoonfar, M. (2015). Finite element modeling and nonlinear analysis for seismic assessment of off-diagonal steel braced RC frame. *International Journal of Concrete Structures and Materials*, 9(1), 89–118.
- Reese, L. C., Cox, W. R. & Koop, F. D. (1974). Field testing and analysis of laterally loaded piles in sand. Proceedings of the VI Annual Offshore Technology Conference, Houston, Texas, 2(OTC 2080): 473–485.
- SAP2000 Version 8. (2002). Basic analysis reference, computers and structures, Inc., Berkeley.
- Scott, B. D., Park, R., & Priestley, M. J. N. (1982). Stress–strain behavior of concrete confined by overlapping hoops at low and high strain rates. *ACI Journal*, 79, 13–27.
- Yingcai, H. (2002). Seismic response of tall building considering soil–pile–structure interaction quake engineering and engineering. *Vibration*, 1, 57–65.